

Initial stages of metal encapsulation during epitaxial growth studied by STM: Rh/Ag(100)

S.-L. Chang, J.-M. Wen, and P. A. Thiel

Department of Chemistry and Ames Laboratory, Iowa State University, Ames, Iowa 50011

S. Günther, J. A. Meyer, and R. J. Behm

Abteilung Oberflächenchemie und Katalyse, Universität Ulm, D-89069 Ulm, Germany

(Received 31 August 1995)

We present results of a scanning tunneling microscope (STM) study of Rh/Ag(100) epitaxy, which shows how the surface rearranges toward the more stable encapsulated structure known to form at higher temperatures. At room temperature, Rh growth proceeds via two competing pathways: (i) thermally activated exchange with Ag surface atoms, which leads to increased coordination of the higher surface free-energy metal Rh by Ag atoms, and (ii) nucleation and growth of mixed Rh/Ag adislands. The Ag-Rh interaction also reduces the surface mobility of Ag, e.g., by local pinning of step edges, accompanied by complex step and surface erosion processes.

Recent work shows that intermixing or place exchange in the surface layer(s) occurs in a variety of systems during epitaxial growth, even if the two components are immiscible in the bulk.¹⁻¹⁰ This may or may not be desirable. The possibility afforded by molecular-beam epitaxy (MBE) of obtaining an unusual (and often thermodynamically unstable) juxtaposition of atoms may lead to materials with interesting and important chemical properties.^{11,12} On the other hand, for films of magnetic interest, specifically for layered materials showing the giant magnetoresistance effect, atomically abrupt interfaces are called for.^{13,14} In order to learn how to further control the intermixing process, it is of obvious importance to understand, in as much detail as possible, the atomic scale mechanisms involved. Here we present scanning tunneling microscopy (STM) results which help elucidate these processes for the Rh/Ag(100) system. A study of this system is relevant for its own interesting characteristics, including the prediction of anomalous magnetic properties of an ideal monolayer of Rh on Ag(100),¹⁵ and also as a model system for growth of a high surface free-energy material on a low surface free-energy substrate.

The Rh/Ag(100) system has been studied previously with a variety of surface-sensitive techniques including ion-scattering spectroscopy (ISS), Auger-electron spectroscopy (AES), work function, CO adsorption,⁹ photoelectron spectroscopy,^{9,15} and positron-annihilation-induced AES.¹⁶ The two main experimental observations of importance here are that (i) annealing room-temperature-deposited Rh films to 600 K causes a decrease in the amount of exposed Rh at the surface, and that (ii) sputtering the annealed surface at room temperature causes an increase in the measured amount of exposed Rh. These results have been interpreted in terms of an encapsulated structure in which a few layers of Ag cover the Rh.⁹ Corrected effective-medium (CEM) calculations corroborate that, indeed, a sandwich-type structure is energetically favorable.¹⁷ Additionally, by performing molecular-dynamics simulations with the energies obtained from the CEM calculations, the kinetics of encapsulation have been explored.¹⁷ The main result of this theoretical work is that at low-Rh coverages, the Ag atoms can move

out of the terrace and quickly cover the Rh, while a complete and perfect monolayer of Rh on Ag(100) obstructs encapsulation for temperatures up to at least 1000 K.¹⁷ In the present study it is shown, by direct STM observation, that at room temperature the formation of the encapsulated structure is thermodynamically favorable but kinetically hindered. The system moves toward the energetically favored configuration by (i) Rh-Ag place exchange, and by (ii) the development of mixed Ag/Rh islands on the terraces, via nucleation and growth from Ag and Rh adatoms moving on the terraces. It is also shown that the mobility of Ag decreases with increasing Rh coverage. This creates a complex competition between what is energetically preferred and what is kinetically possible.

The experiments are carried out in a stainless-steel ultrahigh-vacuum chamber equipped with a home-built pocket-size STM (Ref. 18) and other facilities for surface characterization, i.e., low-energy electron diffraction (LEED), Auger electron spectroscopy (AES), and a mass spectrometer for residual gas analysis. The base pressure is better than 1.1×10^{-8} Pa after bakeout, and rises to 2.5×10^{-8} Pa during evaporation. During the STM data-acquisition process, the pressure is maintained at 1.2×10^{-8} Pa or lower. The Ag sample (1 cm in diameter and 1 mm thick) is oriented and cut to within 0.5° of the (100) direction, and polished to a mirror finish on one side. It is mounted on a molybdenum sample holder fixed by two Ta ribbons in order to transfer between the preparation stage and the STM. Repeated cycles of argon-ion sputtering (30 min, 500 eV, $2.5\text{--}5.0 \mu\text{A}/\text{cm}^2$ at 400 K) and annealing to 900 K are used to remove all impurities, mainly sulphur, carbon, and oxygen, from the surface. The final cleanness of the surface is checked by both AES and STM. No oxygen treatments are used in the cleaning procedures to avoid subsurface oxide formation. After these treatments, the surface shows no detectable contaminants by AES, and atomically flat terraces, on the order of 1000–3000 Å wide with smooth step edges, are frequently obtained.

Rh is evaporated from a source which has been described previously.⁹ The distance from the source to the sample is 10

cm. The evaporation rate is determined by STM evaluation of Rh films deposited on Ru(0001), where no intermixing occurs. The Rh coverage on Ag(100) is calculated from the evaporation times, and checked qualitatively by measuring the peak-to-peak height of the *MNN* Rh Auger transition (at 222 eV). For these experiments, the typical flux is 0.50 ML/min (1 ML is defined as 1.20×10^{15} atoms/cm²). All STM images are acquired at room temperature, starting about 1 h after deposition, and are shown here in a topview representation, with the lighter coloring representing higher features.

We start by giving an overview of the evolution of the film morphology in the low-coverage regime, up to 1.3 ML

[Figs. 1(a)–1(h)], upon room-temperature deposition of increasing amounts of Rh. The clean Ag(100) surface [Fig. 1(a)] displays smooth step edges with the expected monolayer step height of 2.05 Å. Higher-resolution images of the clean surface reveal that the step edges have a “frizzy” appearance, in good agreement with earlier observations on similar surfaces.¹⁹ As can be seen in Fig. 1(b), deposition of 0.02 ML of Rh creates small white islands, and pointlike defects (see inset). Furthermore the step edges begin to roughen. The height of the small islands is the same as that of the Ag(100) step edges, with a density around 6.3×10^{11} cm⁻². The appearance of the defects, which are seen as dark

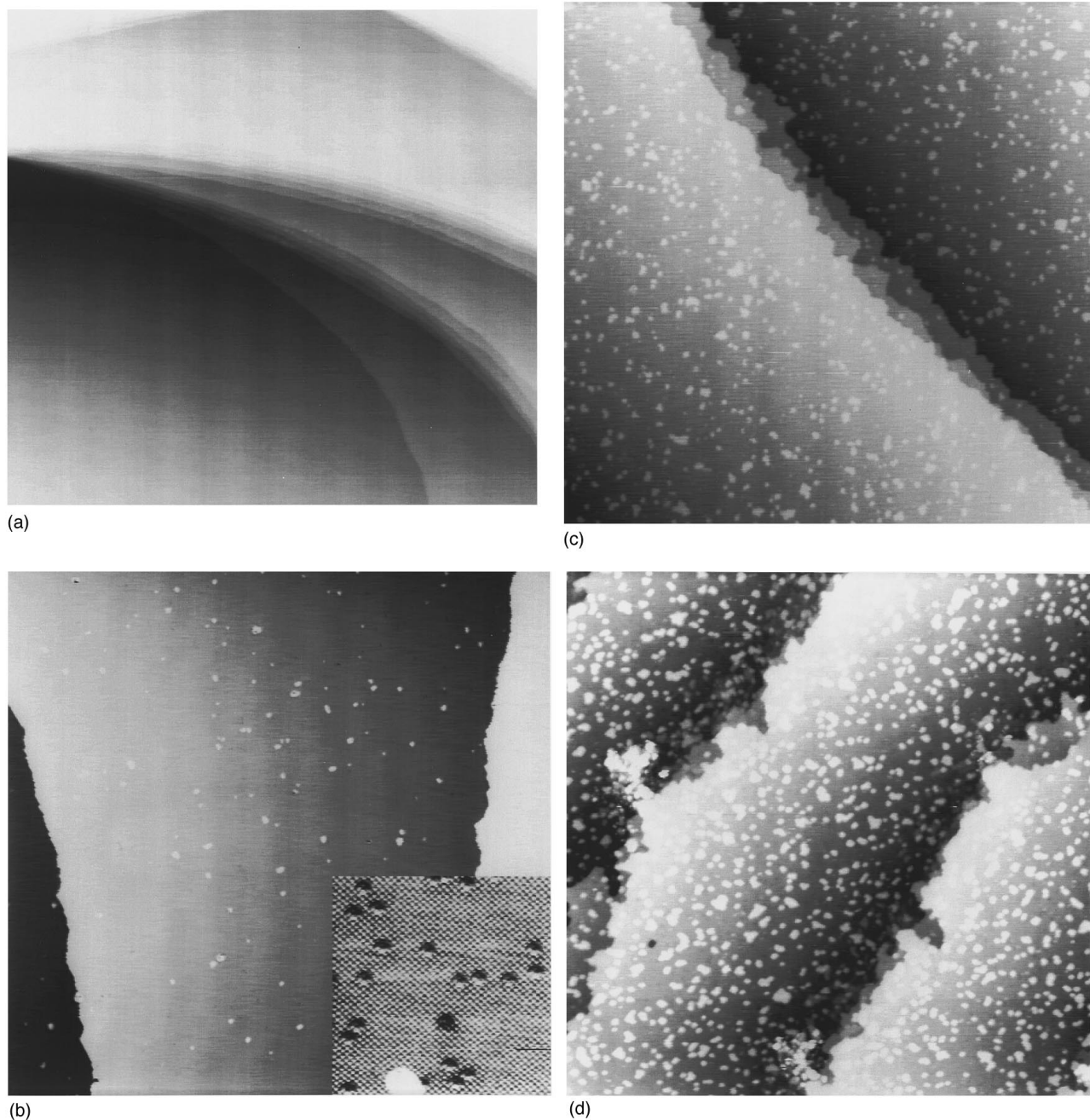


FIG. 1. Sequence of large-scale STM images as a function of increasing Rh coverage on Ag(100) (deposition temperature 300 K). For all coverages adislands as well as substitutional Rh atoms are seen. The step edges becoming increasingly rough up to coverages of 0.50 ML. At this coverage holes in the terraces are seen. (a) Clean surface. (b) 0.02 ML. (c) 0.13 ML. (d) 0.22 ML. (e) 0.36 ML. (f) 0.50 ML. (g) 0.75 ML. (h) 1.3 ML. All images are 150×150 nm² in size, except (a) (250×250 nm) and the inset in (b) (12×12 nm²).

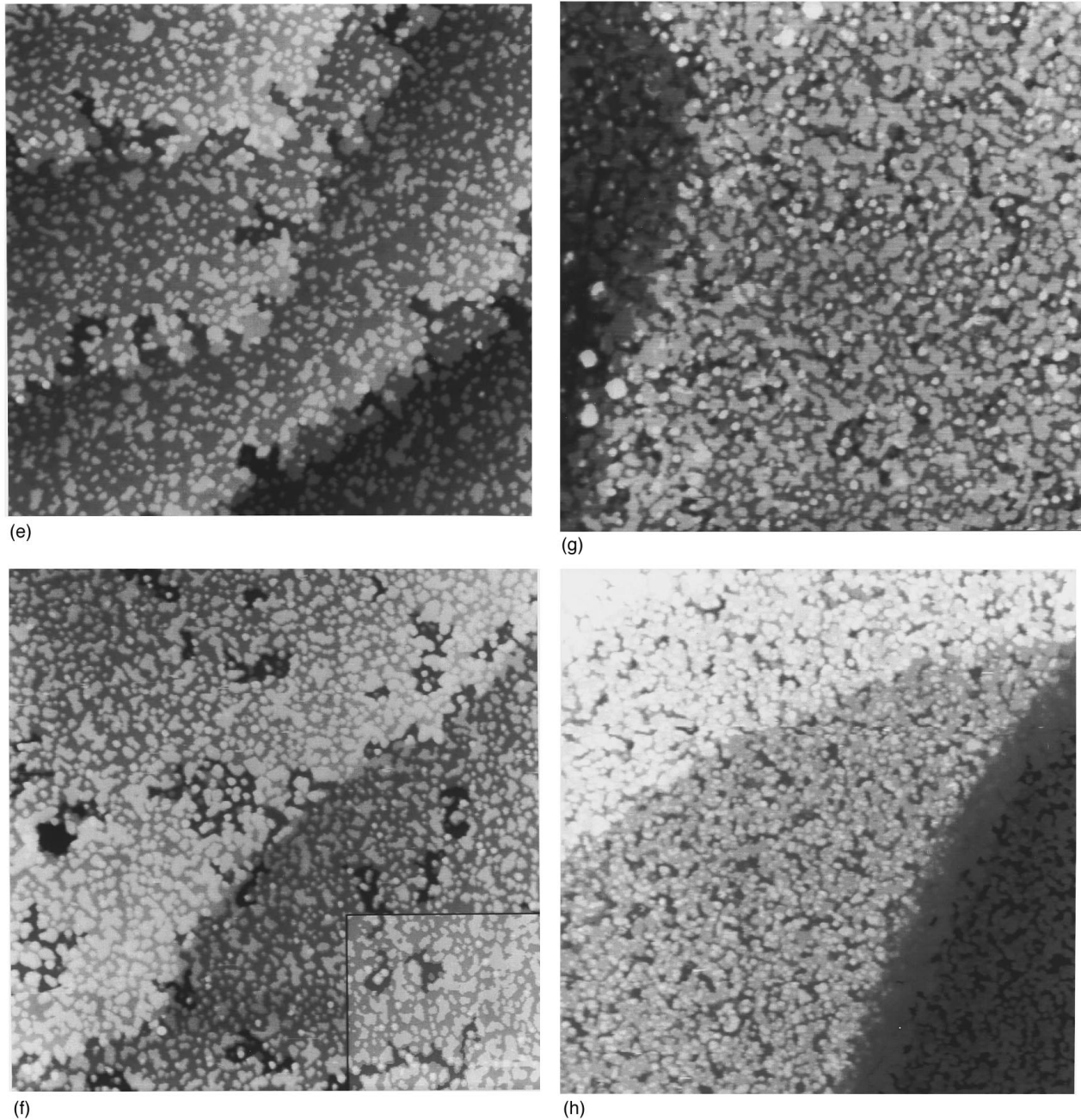


FIG. 1. (Continued).

depressions in the inset in Fig. 1(b), depends on the tip and tunneling conditions; in the experiments here they are measured to be between -0.32 \AA and $+0.78 \text{ \AA}$ high. For 0.02-ML coverage their density is around $1.1 \times 10^{13} \text{ cm}^{-2}$. These defects are assumed to be Rh atoms which have undergone place exchange with substrate atoms. Arguments supporting this hypothesis are given below. The pronounced effects of the imaging conditions on the apparent size of the Rh atoms in the STM images indicates that this is largely determined by electronic effects rather than reflecting the size difference between Ag and Rh.

The monolayer-high islands and the small defects are also observed for higher Rh coverages. With increasing coverage both the average island size and density increase to 20 \AA and $3.0 \times 10^{12} \text{ cm}^{-2}$ at $\theta = 0.13 \text{ ML}$ [Fig. 1(c)], $50\text{--}70 \text{ \AA}$ and 4.6

$\times 10^{12} \text{ cm}^{-2}$ at $\theta = 0.22 \text{ ML}$ [Fig. 1(d)], and 70 \AA and $7.1 \times 10^{12} \text{ cm}^{-2}$ at $\theta = 0.36 \text{ ML}$ [Fig. 1(e)]. Their height, in contrast, does not change. At the same time the step edges become increasingly rough. This change in the step morphology can be caused by either adding or removing material. From Figs. 1(b) and 1(c) it cannot be decided from the appearance of the step edges which of these two possibilities is correct. However, looking at a step edge which is pinned by an impurity makes it clear in which direction the Ag flows. This is demonstrated in Fig. 1(d) for a Rh coverage of 0.22 ML. The thin band of Ag extending out of the step edge to the defect indicates that the step edge has been etched away as a result of Rh deposition. At 0.36 ML [Fig. 1(e)] the step edges have developed a pronounced etched appearance, with a number of irregularly shaped fjords reaching deeply into

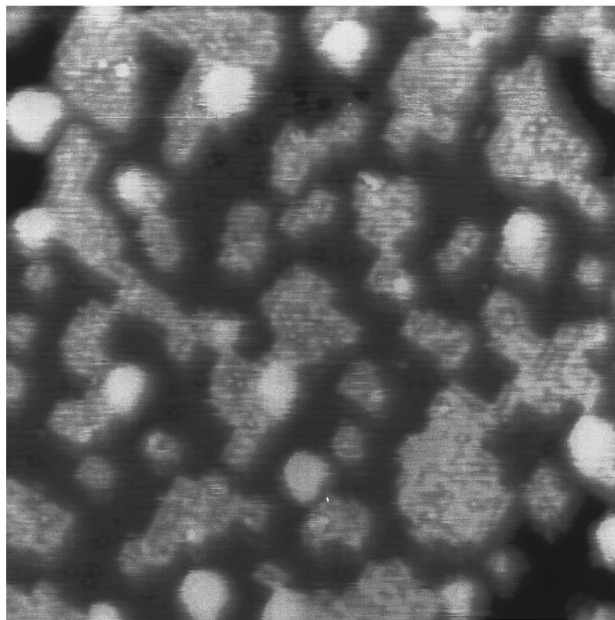


FIG. 2. Higher-resolution image of a Ag(100) surface with 0.75 ML of Rh ($30 \times 25 \text{ nm}^2$). The substitutional Rh atoms are seen here as dark rings. These features can be seen here in three layers, in the holes, the original substrate terraces, and adislands (see the text).

the upper terrace area. Additionally, the adlayer islands have begun to coalesce, and we find second-layer island nucleation (in fact, both of these processes start already around 0.25 ML). The second-layer islands often appear along the top of first-layer island step edges, but apparently there is no strict correlation between the size of the first-layer islands and second-layer nucleation.

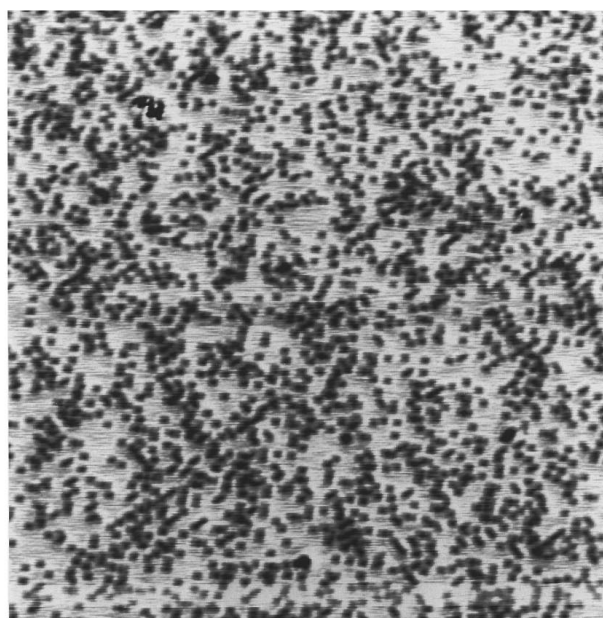
At 0.50 ML of added Rh we observe another phenomenon; small holes eroded into the topmost layer. Also, the irregularly shaped fjords reaching from step edges into the upper terrace become more pronounced [Fig. 1(f)]. The number of second-layer islands has increased, and they appear with higher density near holes in the terrace. Nevertheless, the total population of the second layer is small, around 0.02 ML. At yet higher coverages (0.75 and 1.3 ML) the terraces are covered by many irregularly shaped holes, while etching at step edges is less noticeable; i.e., the etched regions are almost homogeneously distributed over the surface [Figs. 1(g) and 1(h)]. In addition, despite a further increase in second-layer population, the first layer is not yet filled, leaving open channels down to the substrate. The overall morphology of these films indicates that growth has taken place under conditions of kinetically limited interlayer transport, where nucleation of subsequent layers is observed before the underlying layer is filled.

The structural details are better visible in the higher resolution image in Fig. 2, recorded after deposition of 0.75 ML of Rh. There are four layers exposed in this image: the monolayer holes in the substrate (small black regions at top left and bottom right), the original substrate surface (dark grey), first-layer islands (light gray), and finally second-layer islands (white). At this magnification the fourfold symmetry of the substrate becomes more easily seen in the shape of the first-layer islands. (More complicated island shapes result

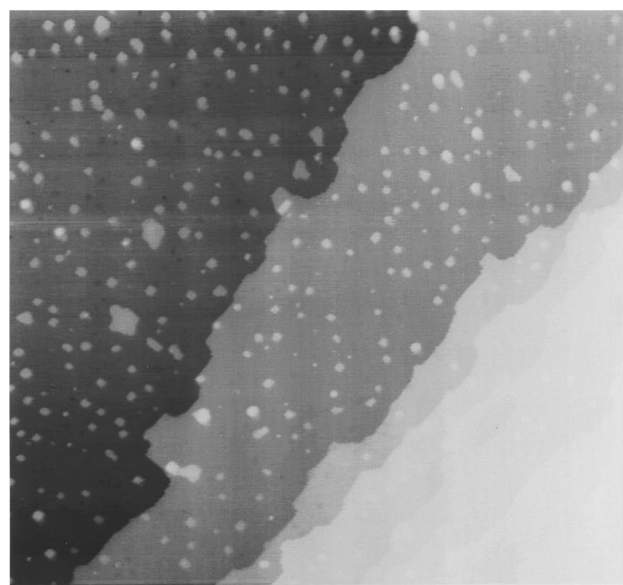
from coalescence of several individual islands.) The pointlike defects in the substrate, shown in the inset of Fig. 1(b), are also seen in this image. Due to different tunneling conditions these are imaged here as very distinct dark rings surrounding slightly elevated circle. These features are not only seen in the substrate, but also in the first-layer islands and the holes. Following our above interpretation, this indicates that all of these layers consist of a mixture of Ag and Rh atoms. (The second-layer islands may also be of mixed composition, but, due to the small size of these, the dark rings are not seen clearly.)

The final experiments to be discussed here deal with the effects of elevated temperatures, either by Rh deposition at elevated temperatures [Fig. 3(a)] or by room-temperature deposition and subsequent annealing [Fig. 3(b)]. Figure 3(a) shows an image of a surface prepared by deposition of 0.36 ML of Rh on a surface held at 500 K. Clearly this leads to a surface different from the one produced by room-temperature deposition [Fig. 1(e)]. The pointlike defects (black spots) are similar to those shown previously [inset in Fig. 1(b)], but their density is much higher now ($1.1 \times 10^{14} \text{ cm}^{-2}$). Furthermore, there no longer exist any first-layer islands on the surface. If there are no other sites to accommodate the deposited Rh atoms, this means that, on average, each of the square defects contains about 4–5 Rh atoms. In contrast, after deposition of 0.30 ML at room temperature and subsequent annealing at 600 K, adlayer islands are still observed, though their density is reduced by the annealing step to about $2.2 \times 10^{12} \text{ cm}^{-2}$.

The above data are understood in terms of two main ideas: (i) Rh atoms are not confined to the adlayer but can exchange with the substrate surface atoms, and (ii) incorporated Rh atoms do not act as perfect traps for diffusing adatoms but do reduce the mobility of diffusing species. At room temperature, deposited Rh atoms can be accommodated either by undergoing a place exchange process with substrate atoms [see the inset to Fig. 1(b)] or by forming adlayer islands of mixed Rh/Ag composition. Comparison of Figs. 3(a) and 1(e), which show a much higher density of substitutional Rh for high-temperature than for room-temperature deposition, makes it clear that this Rh-Ag place exchange is an activated process which competes with migration and eventual island formation. In a simple picture the thermodynamic driving force for this exchange process lies in the higher surface free energy of the Rh deposit, which is also responsible for the formation of stable Ag/Rh/Ag(bulk) encapsulated structures at higher temperatures.⁹ Hence the exchange of Rh adatoms with Ag surface atoms can be viewed as a first step toward these stable encapsulated structures, where the Rh layer is blanketed by a Ag cover layer. The exchange Rh atoms will change the local potential for migrating Rh or Ag adatoms, but not to a degree that they can serve as traps as has recently been reported, e.g., for Ni/Ag(111).⁸ This is supported by data not shown here, where on narrow terraces exchange is still observed, while no or very few adlayer islands can be seen on the same terrace. Finally, the exchanged Rh atoms are immobile at 300 K, while the Ag atoms liberated in the exchange process can migrate over the surface. Furthermore the Rh adatoms can be incorporated at Ag step edges and locally stabilize these; i.e., they effectively act as pinning sites in the other-



(a)



(b)

FIG. 3. Temperature effects on growth and stability of the Rh-covered Ag(100) surface. (a) STM image of a surface prepared by evaporation of 0.36-ML Rh on a 500-K surface ($40 \times 40 \text{ nm}^2$). (b) Image of a surface after evaporation of 0.30-ML Rh with the sample at room temperature, and subsequent annealing to 600 K ($17 \times 17 \text{ nm}^2$).

wise mobile Ag step edges.¹⁹ In this context it should be kept in mind that at room temperature the Ag(100) surface is by no means static but exhibits a significant amount of mobility.²⁰

This leads to the following scenario for Rh growth: The starting Ag surface, at room temperature, is covered by a dilute layer of Ag adatoms on extended flat terraces: e.g., there exists some equilibrium two-dimensional (2D) gas of Ag. The first Rh atoms to arrive at the surface have a rela-

tively high probability of undergoing place exchange, since the nearest island and step edges, which could act as traps, are rather far away. On the other hand, both the deposited Rh adatoms which have not undergone place exchange as well as the exchanged Ag atoms contribute to the density of the adlayer gas. When the density of this mixed 2D gas reaches a critical value (which, among other things, is determined by the adatom mobilities and may also depend on the coverage of underlying substitutional Rh atoms), nucleation of islands becomes likely. In a manner analogous to nucleation and growth in a single species adlayer, islands can nucleate in this adlayer and subsequently grow by incorporation of migrating adatoms hitting the island edges, with the only difference being that in this case the islands are of mixed composition. (Under the experimental conditions used here, this nucleation threshold must be reached at Rh coverages below 0.02 ML, since that is the lowest coverage at which we made measurements, and even there the nucleated islands are already visible.) With increasing coverage the latter process becomes more important, until at a certain coverage the island density has become sufficiently high so that Rh adatom exchange becomes unlikely. For similar reasons nucleation of additional adlayer islands also stops at a certain coverage, and the adisland density saturates. While the islands are not nucleated by exchanged Rh atoms, our data indicate that during subsequent (lateral) growth they overgrow these atoms.²¹

The density of the Rh/Ag islands is about an order of magnitude higher than for Ag/Ag(100).²⁰ In the picture of simple nucleation theory,²² this indicates that the effective mobility of the mixed adlayer on a Ag(100) surface with incorporated Rh atoms is significantly lower than that of Ag adlayer on the clean Ag(100) surface. A similar reduction of the overall mobility had been observed experimentally, and deduced from *ab initio* calculations for Ag(111) homoepitaxy in the presence of Sb surfactant atoms.^{23–25}

At the same time that Rh-Ag islands form, the substrate undergoes complementary morphological changes. Specifically, the steps roughen, starting at 0.02 ML, until by 0.30 ML, fjordlike vacancy structures extend from the step edges. At still higher coverage, 0.50 ML, monolayer holes (vacancy islands) appear also in the middle of terraces. In a separate paper, we will discuss these phenomena and relate them to the formation of vacancy clusters on Ag terraces, from mobile vacancies in the Ag surface layer.

In summary we have shown how for room-temperature Rh deposition the Rh/Ag(100) system evolves toward the energetically favored Ag/Rh/Ag(bulk) structure, namely by an activated exchange of Rh adatoms with Ag surface atoms leading to immobile Rh atoms in the Ag surface layer. The situation is complicated by the simultaneous nucleation and growth of mixed Rh/Ag adlayer islands, where the Ag atoms are provided by exchange, detachment from Ag step edges, and Ag surface erosion. The thermodynamic driving force for this exchange process is attributed to the higher surface free energy of the Rh deposit, also responsible for the formation of stable Ag/Rh/Ag(bulk) encapsulated structures at higher temperatures. For very low coverages most of the deposited Rh undergoes place exchange, and the liberated Ag atoms move to step edges. At intermediate coverages

place exchange is usurped by the formation of Rh-Ag islands; these act as sinks for Ag atoms, causing first erosion at Ag step edges and then erosion of holes in terraces. Upon deposition at elevated temperatures (500 K) the exchange process dominates, demonstrating that this is an activated process.

This work was supported by the IBM Corporation within the Shared University Research (SUR) program (Contract No. 861) and by the National Science Foundation under Grant Nos. INT9213987, CHE-9317660, and GER-9024358. We are grateful for support from the Alexander von Humboldt Foundation (J.A.M.).

-
- ¹S.-L. Chang and P. A. Thiel, *Crit. Rev. Chem.* **3**, 239 (1994), and references therein.
- ²E. I. Altman and R. J. Colton, *Surf. Sci. Lett.* **304**, L400 (1994).
- ³D. D. Chambliss, R. J. Wilson, and S. Chiang, *J. Vac. Sci. Technol. A* **10**, 1993 (1992).
- ⁴S. Rousset, S. Chiang, D. E. Fowler, and D. D. Chambliss, *Phys. Rev. Lett.* **69**, 3200 (1992).
- ⁵K. E. Johnson, D. E. Fowler, and D. D. Chambliss, *Phys. Rev. Lett.* **11**, 1654 (1993).
- ⁶T. Detzel, N. Memel, and T. Fauster, *Surf. Sci.* **293**, 227 (1993).
- ⁷L. P. Nielsen, F. Besenbacher, I. Stensgaard, E. Laegsgaard, C. Engdahl, P. Stolze, K. W. Jacobsen, and J. K. Nørskov, *Phys. Rev. Lett.* **71**, 754 (1993).
- ⁸J. A. Meyer and R. J. Behm, *Surf. Sci. Lett.* **332**, L275 (1995).
- ⁹P. J. Schmitz, W.-Y. Leung, G. W. Graham, and P. A. Thiel, *Phys. Rev. B* **40**, 1 (1989).
- ¹⁰E. S. Hirschorn, D. S. Lin, E. D. Hansen, and T.-C. Chiang, *Surf. Sci. Lett.* **323**, L299 (1995).
- ¹¹J. H. Sinfelt, *Bimetallic Catalysis* (Wiley, New York, 1983).
- ¹²J. A. Rodriguez and D. W. Goodman, *Surf. Sci. Rep.* **14**, 1 (1991), and references therein.
- ¹³S. S. S. Parkin, N. More, and K. P. Roche, *Phys. Rev. Lett.* **64**, 2304 (1990); S. D. Bader and C. Lu, *J. Vac. Sci. Technol. A* **9**, 1924 (1991).
- ¹⁴M. T. Kief and W. F. Egelhoff, Jr., *Phys. Rev. B* **47**, 10 785 (1993), and references therein.
- ¹⁵H. Li, S. C. Wu, D. Tain, Y. S. Li, J. Quinn, and F. Jona, *Phys. Rev. B* **44**, 1438 (1991).
- ¹⁶G. Yang, S. Yang, J. H. Kim, K. H. Lee, A. R. Koymen, G. A. Mulhollan, and A. H. Weiss, *J. Vac. Sci. Technol. A* **12**, 411 (1994).
- ¹⁷T. J. Raeker, D. E. Sanders, and A. E. DePristo, *J. Vac. Sci. Technol. A* **8**, 3531 (1990).
- ¹⁸E. Kopatzki, S. Günther, W. Nichtl-Pecher, and R. J. Behm, *Surf. Sci.* **284**, 154 (1993).
- ¹⁹M. Poensgen, J. F. Wolf, J. Frohn, M. Giesen, and H. Ibach, *Surf. Sci.* **274**, 430 (1992).
- ²⁰J.-M. Wen, S.-L. Chang, J. W. Burnett, J. W. Evans, and P. A. Thiel, *Phys. Rev. Lett.* **73**, 2591 (1994).
- ²¹S.-L. Chang, J.-M. Wen, P. A. Thiel, S. Günther, A. Hitzke, J. A. Meyer, and R. J. Behm (unpublished).
- ²²J. A. Venables, G. D. Spiller, and M. Hanbücken, *Rep. Prog. Phys.* **47**, 399 (1984).
- ²³S. Oppo, V. Fiorentini, and M. Scheffler, *Phys. Rev. Lett.* **71**, 2437 (1993).
- ²⁴J. Vrijmoeth, H. A. van der Vegt, J. A. Meyer, E. Vlieg, and R. J. Behm, *Phys. Rev. Lett.* **72**, 3843 (1994).
- ²⁵J. A. Meyer and R. J. Behm, *Phys. Rev. Lett.* **73**, 364 (1994).